

## Control of metal-directed self-assembly by metal–amine interactions†

Evgeny A. Katayev\* and Markus B. Schmid

Received 18th August 2010, Accepted 6th December 2010

DOI: 10.1039/c0dt01056a

The complexation of a tweezers ligand with zinc perchlorate in the absence and presence of amines in methanol solution was explored.  $L_2Zn_2(ClO_4)_4$  was a thermodynamic product of the reaction in the absence of an amine. The complex was shown to interact with aliphatic amines resulting in the formation of a Zn–N(amine) bond. If metal–ligand complexation was carried out in the presence of an amine the formation of a trinuclear zinc complex  $L_3Zn_3^{6+}$  was observed. Moreover the transformation of complex  $L_2Zn_2^{4+}$  to  $L_3Zn_3^{6+}$  occurred, when the former was subjected to an amine in the amount, which is sufficient to coordinate more than one amino group on each zinc atom. Complexes ligand–zinc–amine were shown to be kinetically stable, and the method of their preparation was crucial to the purity of the final complexes.  $L_3Zn_3^{6+}$  was favored under kinetic control: reagent concentration  $10^{-5}$  M, slow addition of zinc perchlorate to the mixture of an amine and the ligand. Under thermodynamic control (fast mixing of reagents, concentration  $10^{-2}$ – $10^{-3}$  M) formation of a mixture of complexes was observed. All pure complexes and their mixtures were characterized using UV-Vis, ROESY, PFGSE NMR and ESI-MS techniques. On the basis of DFT calculations the mechanism of influence of an amine on self-assembly was suggested.

## Introduction

Using metal coordination as a tool for the self-assembly of organic ligands has attracted considerable attention during the last decade. A vast collection of polynuclear cyclic complexes has been generated with the help of metal-directed self-assembly through N-, P- and O-metal dative bonds.<sup>1–4</sup> The investigation of host–guest chemistry of these molecules has revealed a number of interesting properties such as selective molecular recognition,<sup>5</sup> kinetic stabilization of molecules,<sup>6–8</sup> acceleration of various reactions, thus functioning as molecular flasks.<sup>9</sup> The geometry of a complex is usually pre-programmed in the symmetry of rigid organic ligands. In cases where several cages are possible, it is rather difficult to converge self-assembly into a selective process. However, several methods of controlling metal-directed self-assembly have been found. Gradual addition of reaction components can lead to stepwise growth of intermediates and hence one product.<sup>10–11</sup> Template effects were observed in the guest-dependent formation of MOFs,<sup>12–16</sup> crystallization processes,<sup>17</sup> metal counter-anion dependent self-assembly,<sup>3,18</sup> and templation through  $\pi$ – $\pi$ -stacking interactions.<sup>19–22</sup> Steric effects of bridging<sup>20–23</sup> and supporting ligands<sup>24–26</sup> also may have a crucial role in determining the nuclearity of self-assembled products. We are currently interested in the application of the above mentioned effects in sensing purposes of

functional groups present in biological compounds, in particular amino-groups. Amino-groups being strongly interacting with transition metal centres, may have an influence on self-assembly while present in solution. To our knowledge this has not been investigated in detail. In order to find whether this is possible, one has to design the ligand in a way that it self-assembles in the presence of a metal cation and the resulting complex can interact with amines. Accordingly ligand **1** was designed so that it can coordinate zinc cations in a 2 : 2 stoichiometry.<sup>27</sup> Amide groups play the role of additional intramolecular coordinating ligands, however, due to their weak interaction with zinc they allow the resulting complex to bind amines *via* a substitution mechanism. The coordination of an external amine to zinc may compete with complex formation thereby enabling different pathways of self-assembly. In this work we show that a certain amount of an amine present in solution indeed determines the final structure of the self-assembled complex and can even induce the ring expansion of a cyclic metal complex, namely the transformation of  $L_2Zn_2^{4+}$  to  $L_3Zn_3^{6+}$ . Owing to the kinetic stability of the complexes one can prepare different structures under kinetic control by slow addition of zinc perchlorate to a mixture of an amine and the ligand.

## Results and discussion

## Interaction of zinc complex with amines

Amines are known to coordinate to metal complexes of porphyrins,<sup>28–29</sup> salphens<sup>30–31</sup> and cyclenes<sup>32</sup> among others. Therefore in the design of the ligand (L) we have used aminopyridine fragments<sup>33–34</sup> responsible for zinc ion coordination, and the rigid

Institut für Organische Chemie, Universität Regensburg, Universitätsstr. 31, 93040, Regensburg, Germany. E-mail: evgeny.katayev@chemie.uni-r.de; Tel: 49 941 9434628

† Electronic supplementary information (ESI) available. See DOI: 10.1039/c0dt01056a

2,5-diamidopyrrole unit<sup>35–36</sup> that separates metal binding sites to exclude 1:1 complex formation. First, we have studied the complexation of L with zinc perchlorate in methanol solution and its binding properties towards aliphatic monoamines and diamines. According to the UV-vis titration complex  $L_2Zn_2^{4+}$  is formed in a stepwise manner with  $\log\beta_{12} = 9.98(5)$  and  $\log\beta_{22} = 13.16(7)$ . X-ray single crystal analysis has proven that the amide oxygens are coordinated to zinc and form a hexagonal coordination sphere together with 2-aminomethylpyridine residues, thereby positioning the pyrrole rings almost parallel to each other (Fig. 1). Interestingly, such a coordination takes place in solution, too: In the  $^1H$  NMR spectrum of  $L_2Zn_2^{4+}$  the methylene protons of L appear as doublets with different chemical shifts, hence they are chemically non-equivalent. From the crystallographic data it is inferred that coordination of the amide oxygen to zinc results in close proximity of one methylene proton to the methyl group of the pyrrole ring (Fig. 1). This is the interaction we found to be the case from 2D-ROESY measurements (*cf.* ESI†).

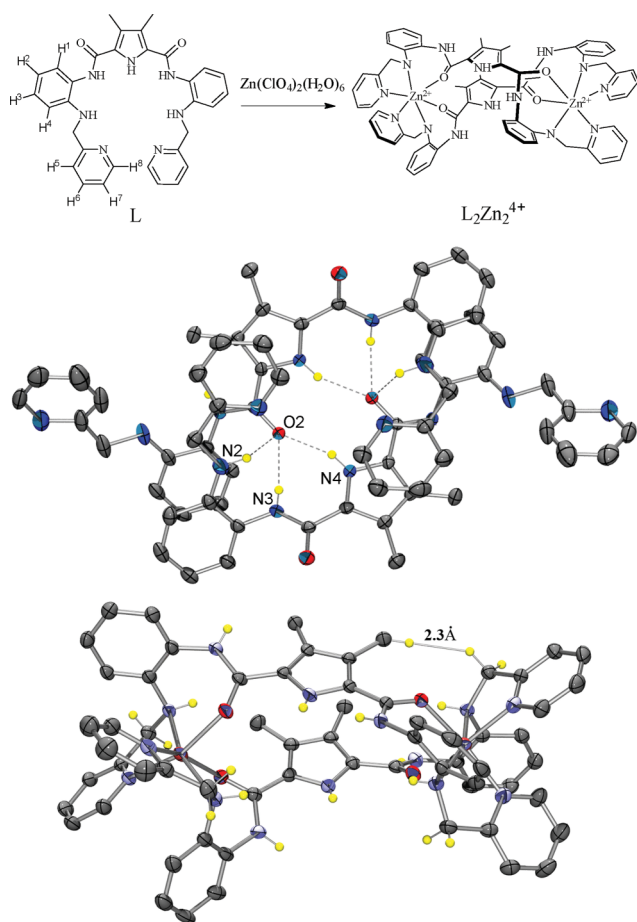


**Fig. 1** Synthesis of complex  $L_2Zn_2(ClO_4)_4$  and X-ray crystal structures of the ligand dimer and the zinc complex. Hydrogen bonds are shown as dashed lines, solvent molecules, perchlorate anions and most of the hydrogen atoms have been omitted for clarity.

According to the UV-Vis measurements the amines (*n*-propylamine,  $NH_2-(CH_2)_n-NH_2$ ,  $n = 2-6$ ) coordinate to the zinc cations through stepwise substitution of the Zn–O(amide) bond to the Zn–N(amine) bond. In all cases the complexation was accompanied by similar changes in the UV-vis spectrum: increase

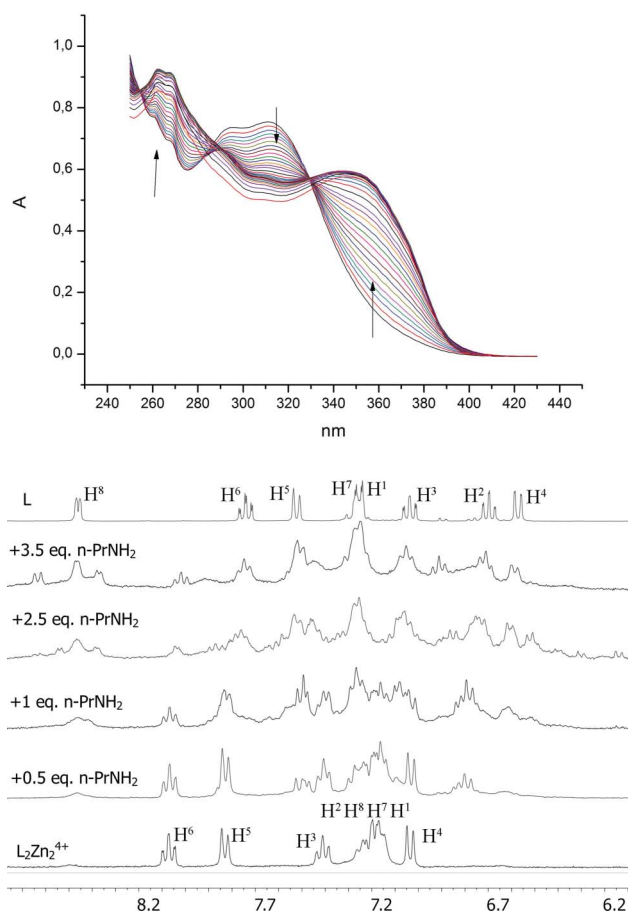


**Fig. 2** Characteristic spectrophotometric changes which are observed upon addition of an amine to  $L_2Zn_2(ClO_4)_4$  ( $c = 10^{-5}M$ ) in methanol.  $^1H$  NMR titration of the complex with *n*-propylamine ( $n-PrNH_2$ ,  $c = 4 \times 10^{-3}M$ ).

at 350 nm and decrease at 310 nm bands (Fig. 2). From the first binding event it was clear that monoamines coordinate in a 1:2, while diamines coordinate in a 1:1 stoichiometry (Tab. 1). The second binding event was also observed, however its curvature was not sufficient to extract data with sufficient accuracy. Interestingly, ethylenediamine (the shortest diamine) binds to  $L_2Zn_2^{4+}$  in a similar manner (1:2 stoichiometry) as monoamines, however addition of more than 6 equivalents led to the transformation of the absorbance spectrum to that of the ligand. On this basis, it was concluded that an excess of ethylenediamine moves the dynamic system towards the formation of the zinc-ethylenediamine complex, which is known to have a higher stability constant.<sup>37</sup>

Because the X-ray single crystal analysis was not available due to the fast decomposition of crystals, information about the mode of the amine interaction with the zinc cation was obtained from NMR measurements.  $^1H$  NMR titration of the complex with *n*-propylamine (Fig. 2) showed that upon addition of the amine up to 1 equiv. the number of signals increases, which is the hallmark of  $L_2Zn_2(n-PrNH_2)^{4+}$  complex formation. Using 2D ROESY three  $CH_2$ (pyridine) fragments were found to interact through the space with aromatic rings and one not, meaning that one zinc center is surrounded by equivalent and conformationally “fixed”  $CH_2$ (pyridine) fragments, and the other zinc center has

**Table 1** Apparent constants for complex formation determined from UV-Vis titrations at 25 °C in methanol solution in the presence of different substrates

| Substrate                              | $\log\beta_{12}$  |
|--|---|
| <i>n</i> -PrNH <sub>2</sub>            | 11.62(7)  |
| ethylenediamine                        | 10.22(2)  |
|  | $\log\beta_{11}$  |
| 1,3-diaminopropane                     | 5.48(2)   |
| 1,4-diaminobutane                      | 6.41(5)   |
| 1,5-diaminopentane                     | 6.20(5)   |
| 1,6-diaminohexane                      | 6.94(3)   |
| without the guest                      | $\log\beta_{21} = 9.98(5)$ ; $\log\beta_{22} = 13.16(7)$    |
| 1 equiv. <i>n</i> -PrNH <sub>2</sub>   | $\log\beta_{21} = 10.71(4)$ ; $\log\beta_{22} = 15.61(4)$   |
| 2 equiv. <i>n</i> -PrNH <sub>2</sub>   | $\log\beta_{32} = 20.88(12)$ ; $\log\beta_{33} = 25.46(12)$ |
| 4.1 equiv. <i>n</i> -PrNH <sub>2</sub> | $\log\beta_{11} = 6.14(8)$ ; $\log\beta_{12} = 11.82(10)$   |
| 0.5 equiv. PDA                         | $\log\beta_{32} = 20.08(10)$ ; $\log\beta_{33} = 24.51(10)$ |
| 1 equiv. PDA                           | $\log\beta_{32} = 20.11(6)$ ; $\log\beta_{33} = 24.88(6)$   |
| 2.1 equiv. PDA                         | $\log\beta_{11} = 5.68(6)$ ; $\log\beta_{12} = 11.10(10)$   |

both flexible and “fixed” fragments. For the first group of signals we still observed CH<sub>2</sub>(pyridine)–Me(pyrrrole) interactions through the space as for the starting complex. Existence of NOE cross-peaks between the propyl-group and aromatic rings (*cf.* ESI†) allowed us to propose the structure of complex L<sub>2</sub>Zn<sub>2</sub>(*n*-PrNH<sub>2</sub>)<sup>4+</sup> (Fig. 3).

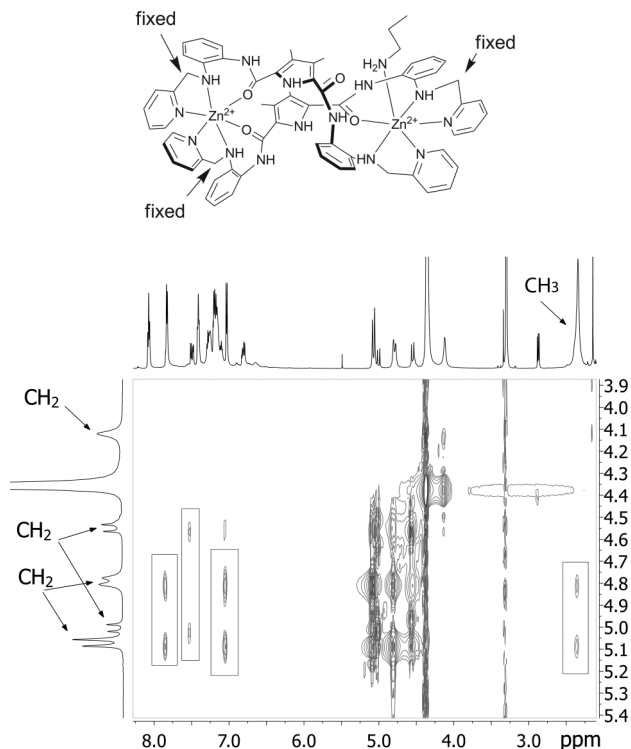


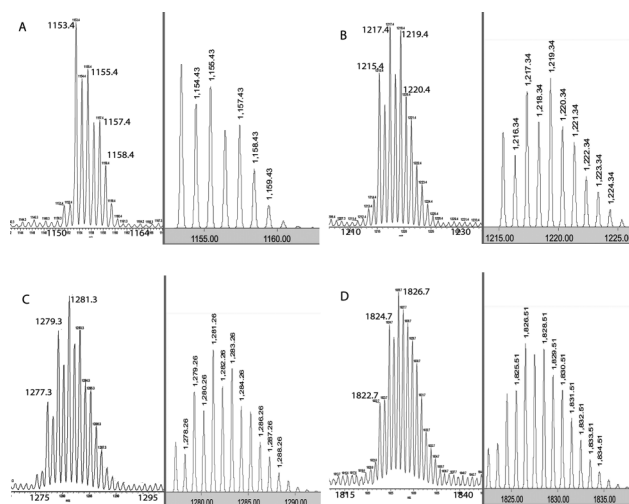
**Fig. 3** Structure of the complex with *n*-PrNH<sub>2</sub> proposed on the basis of 2D-ROESY, the corresponding spectrum is also shown.

From <sup>1</sup>H NMR titration of L<sub>2</sub>Zn<sub>2</sub><sup>4+</sup> with 1,5-pentanediamine (PDA) and *n*-PrNH<sub>2</sub> follows that upon addition of amines in amounts of more than 0.5 and 2 equivalents, respectively, several complexes are formed. Thus, we prepared mixtures of L<sub>2</sub>Zn<sub>2</sub><sup>4+</sup> with

various amounts of *n*-PrNH<sub>2</sub> and PDA using (a) 10<sup>-3</sup>M and (b) 10<sup>-5</sup>M component concentration in methanol and subjected them to ESI-MS analysis.

To our surprise the formation of the large macrocyclic complex L<sub>3</sub>Zn<sub>3</sub><sup>6+</sup> was observed when the above mentioned quantities of amines were used at 10<sup>-3</sup> sample concentration. This transformation is less pronounced when the experiment was carried out at 10<sup>-5</sup>M component concentration. More than 2 equiv. of PDA and 4 equiv. of *n*-PrNH<sub>2</sub> were needed to observe L<sub>3</sub>Zn<sub>3</sub><sup>6+</sup> species in mass spectra.

According to the mass spectra when 1 (*n*-PrNH<sub>2</sub>) or 0.5 (PDA) equivalents of an amine were added to 10<sup>-5</sup> M methanol solution of L<sub>2</sub>Zn<sub>2</sub><sup>4+</sup>, new peaks appeared. These peaks correspond to species [LZn(*n*-PrNH<sub>2</sub>)–H]<sup>+</sup> (*m/z* = 667.4), and [LZn(PDA)–H]<sup>+</sup> (*m/z* = 710.4) respectively. Addition of acetonitrile to the solution of complexes allowed us to observe the exact mass of one of the proposed complexes with amine: [L<sub>2</sub>Zn<sub>2</sub>(PDA)(Cl<sup>-</sup>)–H]<sup>2+</sup> (*m/z* = 677.4, *cf.* ESI†). When 5 equivalents of *n*-PrNH<sub>2</sub> were added to L<sub>2</sub>Zn<sub>2</sub><sup>4+</sup> (*c* = 10<sup>-5</sup>M) the following species in ESI-MS were observed: [LZn–H]<sup>+</sup>, [L<sub>2</sub>Zn<sub>2</sub>–3H]<sup>+</sup>, and [L<sub>3</sub>Zn<sub>3</sub>–5H]<sup>+</sup>. Addition of 3 equivalents of PDA led to the observation of more species: [LZn–H]<sup>+</sup>, [L<sub>2</sub>Zn–H]<sup>+</sup>, [L<sub>2</sub>Zn<sub>2</sub>–3H]<sup>+</sup>, [L<sub>3</sub>Zn–H]<sup>+</sup>, [L<sub>3</sub>Zn<sub>2</sub>–3H]<sup>+</sup> and [L<sub>3</sub>Zn<sub>3</sub>–5H]<sup>+</sup> (Fig. 4).



this question we have conducted a test experiment: measurement of  $^1\text{H}$  NMR and ESI mass spectra of  $10^{-3}\text{M}$  methanol solution of L+PDA in equimolar amounts to which one equivalent of zinc perchlorate in (a) one portion and (b) seven portions was added. From Fig. 5 it can be seen that under thermodynamic control (a) the  $^1\text{H}$  NMR profile resembles the one of the ligand, but the signals are broadened and slightly shifted to higher field. In mass spectrum peaks with masses of  $[\text{LH}]^+$ ,  $[\text{LZn-H}]^+$  and  $[\text{LZn}(\text{PDA})-\text{H}]^+$  dominated (*cf.* ESI $^\dagger$ ). Under kinetic control (b) the  $^1\text{H}$  NMR spectrum is rather complicated, meaning that a number of complexes were generated during the synthesis. Species ranging from mono- to tri-zinc complexes were observed in the mass spectrum. On this basis it is concluded that complexes are kinetically stable and the method of mixing is crucial to the generation of pure complexes.

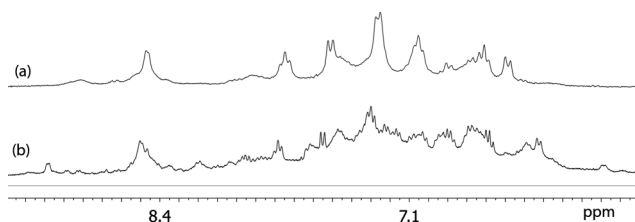


**Fig. 5** Comparison of  $^1\text{H}$  NMR spectra produced by addition of zinc perchlorate (a) in one portion and (b) in seven portions to the equimolar mixture of the ligand and 1,5-pentanediamine in  $\text{CD}_3\text{OD}$  ( $c = 10^{-3}\text{M}$ ).

In order to get closer to ideal kinetic control and to find out if it is possible to generate in these conditions pure complexes, we titrated the mixture of the ligand and an amine with zinc perchlorate, where the concentration of an amine is varied and the apparent stability constant  $\beta_{\text{app}}$  and stoichiometry of ligand–zinc interaction is determined. The results of the titrations in the presence of *n*-PrNH $_2$  and PDA are shown in Table 1 (other diamines except 1,2-ethylenediamines behave similarly). Interestingly, one equivalent of the monoamine and 0.5 equivalents of the diamine (relative to L), the amount which is sufficient to replace one amide oxygen atom on each metal, induced stabilization of the assembly by almost two orders of magnitude in  $\beta_{22}$ . If the guest concentration was high enough to substitute two intramolecular metal–oxygen bonds on each metal, 3 : 2 stoichiometry was observed. The construction of  $\text{L}_3\text{Zn}_3^{6+}$  proceeded through 3 : 2 followed by a 3 : 3 binding event (Tab. 1). The presence of excess of an amine in the solution led to the formation of a complex with a 1 : 2 ligand to zinc stoichiometry ( $\text{LZn}_2^{4+}$ ). An exceptional case is 1,2-ethylenediamine. The presence of 0.5–1 equivalents in the solution resulted in a 3 : 2 stoichiometry of binding with  $\log\beta_{32} = 21.60(12)$  and  $\log\beta_{33} = 25.87(12)$ , however the presence of two equivalents of the diamine resulted in 3 : 4 binding stoichiometry with  $\log\beta_{34} = 32.64(20)$ . The instability of ethylenediamine complexes, namely transformation to the thermodynamically more stable zinc-ethylenediamine complex, complicated further studies with NMR and mass-spectrometry. Thus, among all the diamines studied self-assembly between zinc perchlorate and the ligand “feels” (results in a different stoichiometry of the interacting species) the structural difference only between 1,2-ethylenediamine and other amines. Such a behavior is in agreement with previously reported palladium complexes with sterically different supporting ligands, however

they were prepared under thermodynamic control starting from the palladium complex already bearing the supporting ligand. $^{25}$  In our case building of a complex occurs gradually during the slow addition of zinc perchlorate to the mixture of the ligand and an amine. Thus, the coordination of an amine to zinc cation dictates the ligand orientation in space, thereby enabling alternative ways of self-assembly (3 : 3 or 2 : 2). This assumption also explains the fact that self-assembly “feels” the quantity of an amine present in solution. The different complex compositions were verified by subsequent mass spectrometry analysis of each solution, where either  $[\text{L}_2\text{Zn}_2-3\text{H}]^+$ ,  $[\text{L}_3\text{Zn}_3-5\text{H}]^+$  or  $[\text{LZn}_2-3\text{H}]^+$  were observed.

### $^1\text{H}$ NMR and PFGSE measurements

In order to determine the distribution of species in methanol solution a number of proton NMR spectra of mixtures ligand–zinc–amine were measured. We used our finding that complexes are kinetically stable (Fig. 5) and the fact that it is possible to prepare them in pure form (according to ESI-MS) using diluted conditions ( $10^{-3}\text{M}$ ) as for UV-Vis spectroscopy. Thus, to measure  $^1\text{H}$  NMR of these solutions we used the following technique: after mixing the components under diluted conditions the methanol solution was evaporated at room temperature, dried and the residue was dissolved in 0.5 ml  $\text{CD}_3\text{OD}$ . Three key experiments were conducted from which it was clear what are the dominant species in solution:

- (1) (L+PDA)+0.5Zn – slow addition of 0.5 equiv. of zinc perchlorate to an equimolar mixture of the ligand and PDA;
- (2) (L+PDA)+Zn – slow addition of 1 equiv. of zinc perchlorate to an equimolar mixture of the ligand and PDA;
- (3) (L+2PDA)+2Zn – slow addition of 2 equiv. of zinc perchlorate (relative to L) to the mixture of the ligand and PDA in a 1 : 2 ratio.

All spectra were compared with those of the ligand and of the mixture of  $\text{L}_2\text{Zn}_2^{4+}$  and 3 equiv. of PDA (Fig. 6).  $^1\text{H}$  NMR of the solutions showed that the mixtures consist of 2 major components and one component is present in all cases. Since this component was found in considerable amount under the conditions used to produce  $\text{L}_3\text{Zn}_3^{6+}$  complex ((L+PDA)+Zn, Fig. 6) we assigned the corresponding signals to the trinuclear zinc complex  $[\text{L}_3\text{Zn}_3(\text{PDA})_n]^{6+}$ . Evidently, the major complex formed in conditions (L+2PDA)+2Zn can be assigned to  $\text{LZn}_2(\text{PDA})_n^{4+}$ . Conditions (L+PDA)+0.5Zn were initially carried out as an attempt to prepare  $\text{L}_2\text{Zn}_2^{2+}$  complex, which can be considered as

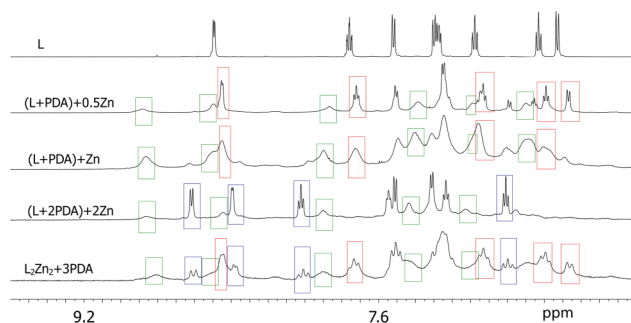


**Fig. 6** Comparison of  $^1\text{H}$  NMR spectra of complexes prepared under different conditions (see text) as  $10^{-3}\text{M}$  solution in  $\text{CD}_3\text{OD}$ . Squares of different colors correspond to a certain compound present in the mixture.

an intermediate in the construction of larger complexes. However, according to Fig. 6 there are only two products in this reactions:  $L_3Zn_3(PDA)_n^{6+}$  and the product that has a signal pattern similar to that of the ligand, but the signals are shifted to higher field. This means that a ligand–zinc interaction is present. The ratio between the trinuclear complex and the other product is 0.5 : 1 respectively, which is lower than statistically predicted (1 : 1), assuming that only  $L_3Zn_3(PDA)_n^{6+}$  and the ligand are formed. Hence, besides the trinuclear complex and the ligand other zinc complexes are present. This fact is in agreement with the ESI-MS spectrum of this mixture, where  $[LH]^+$  and  $[L_2Zn-H]^{2+}$  are the most intensive peaks (*cf.* ESI†).

Accurate analysis of Fig. 6 reveals that addition of more than 2 equiv. of PDA to  $L_2Zn_2(ClO_4)_4$  in methanol indeed induces the transformation of the initial complex to a larger trinuclear zinc complex, and in addition leads to the formation of the complexes  $LZn_2^{4+}$ ,  $L_2Zn^{2+}$  and the ligand. Thus, on the basis of UV-vis titrations coupled with ESI-MS and  $^1H$  NMR measurements we propose 3 possible pathways of self-assembly (Fig. 7).

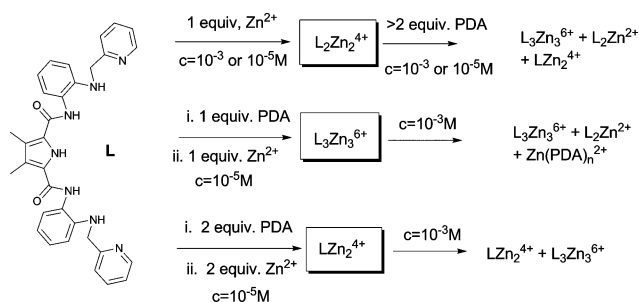


**Fig. 7** Possible pathways of ligand–zinc self-assembly in the absence and presence of the amine in methanol solution. In all cases slow addition of zinc cation was used.  $c = 10^{-3}M$  – stands for concentration of the solution from  $10^{-5}$  to  $10^{-3}M$  (see text).

To provide additional proof for the structures of the species formed as a result of ligand–zinc–amine self-assembly, we carried out PFGSE (pulsed field-gradient spin-echo) NMR measurements in  $CD_3OD$  with total complex concentrations  $10^{-3}M$ . This method allows us to determine the hydrodynamic radii ( $r_H$ ) of molecules present in solution, and thus is especially valuable for the analysis of mixtures of self-assembled complexes.<sup>38</sup> The hydrodynamic radius of the diffusing species can be estimated from the experimentally determined self-diffusion translational coefficient ( $D$ ) by taking advantage of the Stokes–Einstein equation:

$$D = \frac{kT}{c\pi\eta r_H} \quad (1)$$

where  $k$  is the Boltzmann constant,  $T$  is the temperature,  $c$  is a numerical size factor, and  $\eta$  is the solution viscosity. According to Wirtz and co-workers<sup>39</sup>  $c$  is expressed as a function of the solute-to-solvent ratio of radii, and has a non-linear dependence on  $r_H$ , when  $r_H$  is between 3–6 Å range. The radii of species in our work are generally more than 6 Å, hence  $c$  can be considered as constant. Thus, we used a simplified method suggested by Zuccaccia and Macchioni<sup>40</sup> for obtaining accurate  $r_H$  values by carrying out the experiment using TMS (tetramethylsilane) as an internal standard. From eqn (1), the ratio of  $D$  values for the two species is:

$$\frac{D^{sa}}{D^{st}} = \frac{C^{st}r_H^{st}}{C^{sa}r_H^{sa}} \quad (2)$$

where sa and st stand for sample and standard. To determine the unknown parameter  $c^{st}/c^{sa}$  we used the hydrodynamic radius of complex  $L_2Zn_2^{2+}$  taken from crystallographic data and literature known radius of TMS.<sup>41</sup> Table 2 gathers observed  $D$  and  $r_H$  values for the mixtures described previously (Fig. 6). Structures of key complexes were calculated using the DFT method in the program package “Priroda”.<sup>42</sup> The calculated hydrodynamic radii of the

**Table 2** Diffusion coefficients ( $D$ ) and calculated hydrodynamic radii ( $r_H$ ) for the ligand and complexes<sup>a</sup>

| Compound or method of preparation | Compound                    | $D_{obs} \times 10^{-9} / m^2 s^{-1}$ | $r_H / \text{Å}$  | $m/z$  | Assigned products         |
|-----------------------------------|-----------------------------|---------------------------------------|-------------------|--|---------------------------|
| L                                 | TMS                         | 3.29                                  |                   | $[LH]^+$ , 546.6   | L                         |
|                                   | ligand                      | 1.42                                  | 7.86              |  |                           |
| $L_2Zn_2$                         | TMS                         | 3.62                                  | 2.96 <sup>b</sup> | $[L_2Zn_2-3H]^+$ , 1215.3  | $L_2Zn_2^{4+}$            |
|                                   | component1                  | 1.25                                  | 9.87 <sup>b</sup> |  |                           |
|                                   | PDA                         | 1.15                                  | 8.14              |  |                           |
|                                   | TMS                         | 2.18                                  |                   | $[L_2Zn-H]^+$ , 1153.4; $[L_2Zn_2-3H]^+$ , 1215.3; $[L_3Zn_3-5H]^+$ , 1822.7 | $L_c^c$ , $+L_3Zn_3^{6+}$ |
| (L+PDA)+0.5Zn                     | component1                  | 0.56                                  | 13.15             |  |                           |
|                                   | component2                  | 0.53                                  | 14.02             |  |                           |
|                                   | PDA                         | 0.79                                  | 9.43              |  |                           |
|                                   | TMS                         | 2.94                                  |                   | $[L_2Zn-H]^+$ , 1153.4; $[L_2Zn_2-3H]^+$ , 1215.3; $[L_3Zn_3-5H]^+$ , 1822.7 | $L_c$ , $+L_3Zn_3^{6+}$   |
|                                   | component1                  | 0.74                                  | 13.44             |  |                           |
| $L_2Zn_2+n-PrNH_2$                | PDA                         | 1.07                                  | 9.32              |  |                           |
|                                   | TMS                         | 3.71                                  |                   | $[LZn(n-PrNH_2)-H]^+$ , 667.4; $[L_2Zn_2-3H]^+$ , 1215.3                     | $L_2Zn_2^{2+}$            |
|                                   | component1                  | 1.30                                  | 9.70              |  |                           |
|                                   | <i>n</i> -PrNH <sub>2</sub> | 2.56                                  | 4.93              |  |                           |
| (L+2PDA)+2Zn                      | TMS                         | 2.59                                  |                   | $LZn_2(PDA)_2Cl-H]^+$ , 810.2  | $LZn_2^{4+}$              |
|                                   | component1                  | 1.07                                  | 8.21              |  |                           |
|                                   | PDA                         | 1.28                                  | 6.87              |  |                           |
|                                   |                             |                                       |                   |  |                           |

<sup>a</sup> All samples were measured as  $10^{-3}M$  solutions in  $CD_3OD$  at 300 K. The values reported are the average of 2–3 different measurements, which differ by less than 3%. The experimental error is 2%. Standard deviation is *ca.*  $\pm 0.03$  nm. <sup>b</sup> Values used to calculate unknown parameters in eqn (2). <sup>c</sup>  $L_c$  – stands for the mixture of species L and  $L_2Zn^{2+}$ .

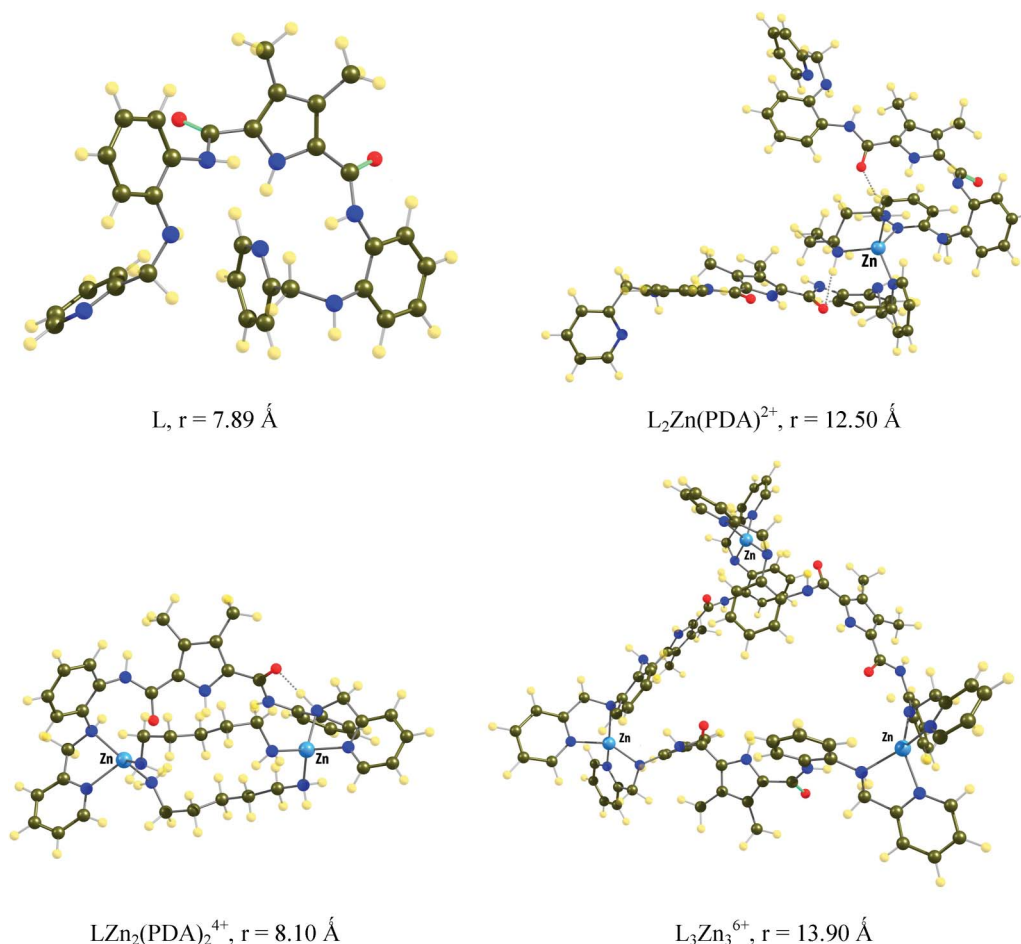


**Fig. 8** Calculated structures and hydrodynamic radii of the ligand and self-assembled complexes. For complex  $L_3Zn_3^{6+}$  one of the possible isomers is shown.

complexes and the ligand are shown in Fig. 8. The observed  $r_H$  values for the ligand and the complexes were in very good agreement with the predicted ones (Tab. 2). Interestingly, the observed  $r_H$  value for the ligand (7.86 Å) is identical to the calculated one (7.89 Å) but is smaller than the one obtained from the solid structure (9.02 Å). This difference can arise from the fact that in the solid state the ligand is dimerized and hence has a larger volume. Complex  $LZn_2(PDA)_2^{4+}$  was calculated with PDA, assuming that coordination of the latter can dramatically decrease the size of the complex. In PFGSE measurements the component separation was observed only for the sample (L+PDA)+0.5Zn (Tab. 2). In sample (L+PDA)+Zn there was no signal separation due to their considerable overlap and we observed an average radius of two species. The component which was assigned in the previous section as a mixture of the ligand and  $L_2Zn^{2+}$  has indeed a larger radius than the ligand and is close to the one of the  $L_2Zn^{2+}$  complex.

#### DFT calculations

The observed “templating” behavior of PDA (and other amines) is an unusual fact. It is appropriate to suggest that the key species that enables the new pathway of self-assembly towards the trinuclear

zinc complex is  $L_2Zn(PDA)_2^{2+}$ , where PDA plays the role of a preorganization element. Since it was not possible to prepare such a complex in pure form and to investigate its structure in solution we conducted DFT calculations. A conformational search of the structure of complex  $L_2Zn(PDA)_2^{2+}$  was carried out by using different starting geometries for the calculations. As a result the conformation depicted in Fig. 8 was the most favorable one. Interestingly, the orientation of the ligands in the complex is stabilized by two hydrogen bonds formed between amide-oxygens and NH-protons of the amine. Thus, coordinated PDA causes the positioning of the rest of the chelating groups in space far from each other (Fig. 9). This can be the reason why a certain amount of an amine induces either reorganization of smaller to larger cyclic complexes or drives the overall self-assembly in a specific way.

#### Conclusions

In conclusion, we designed the ligand specifically for self-assembly with zinc cations and aliphatic amines in methanol solution. The unique structural feature of the ligand is that it forms a complex with zinc cations in a 2 : 2 stoichiometry, which coordinates mono- and diamines *via* substitution of intramolecularly coordinated amide oxygens. The competitive nature of the components (the

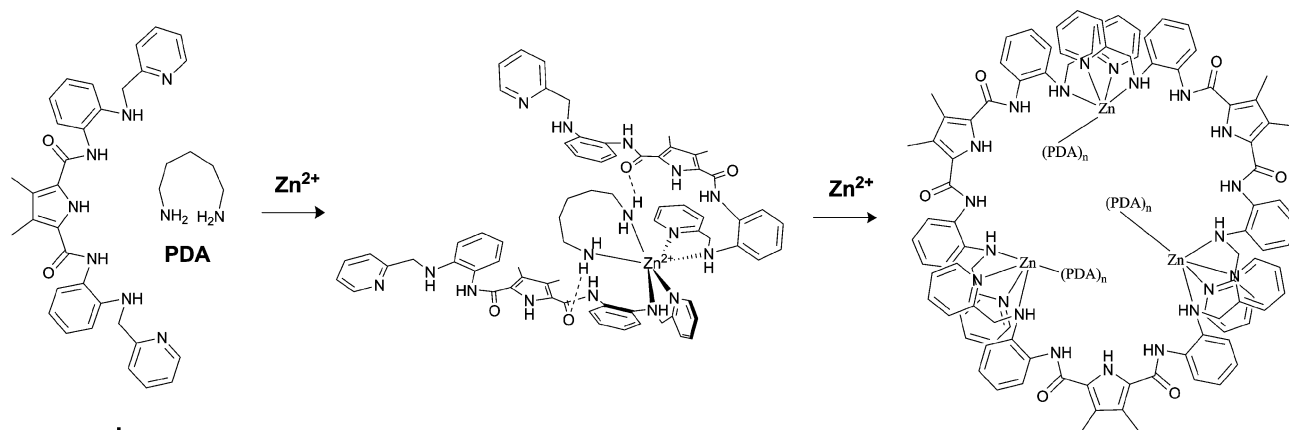


Fig. 9 Proposed mechanism of the formation of  $L_3Zn_3^{6+}$  complex.

ligand and amines) allowed us to direct metal–ligand self-assembly to different di- and even trinuclear zinc complexes. Moreover the transformation of complex  $L_2Zn_2^{4+}$  to  $L_3Zn_3^{6+}$  occurs, when the first is subjected to an amine in an amount, which is sufficient to coordinate one amino group on each zinc atom. DFT calculations suggest that the reason for such a control is that pre-coordination of an amine to the zinc cation dictates the geometry of subsequent ligand coordination. Therefore, alternative paths of self-assembly were possible only under kinetic control of complex formation, namely gradual addition of the components. The complexes described represent a rare example of kinetically stable complexes<sup>43</sup> and methods for control of their assembly are yet to be explored. The design of ligands whose self-assembly with metal cations is sensitive to the guest structure may be regarded as an attractive analytical tool for detection of amine functionalities. Current efforts in this direction are being pursued in our laboratory.

## Experimental

### General methods

All solvents were of reagent grade quality and purchased commercially. All starting materials were purchased from Aldrich, Acros and Fluka Chemical Co. NMR spectra used in the characterization of products were recorded on Bruker Avance 300 instruments. The NMR spectra were referenced to solvent and the spectroscopic solvents were purchased from Cambridge Isotope Laboratories. Mass spectra were recorded with Finnigan MAT SSQ 710 A (CI) and Finnigan MAT 95 (HRMS). Column chromatography was performed on Whatman silica gel 60 Å (230–400 mesh). UV/Vis spectra were recorded on a Cary BIO 50 UV/Vis/NIR spectrometer (Varian).  $N^2,N^3$ -bis(2-aminophenyl)-3,4-dimethyl-1*H*-pyrrole-2,5-dicarboxamide has been synthesized according to the published procedure.<sup>44</sup>

### Titration conditions

Stock solution with concentrations of  $10^{-5}$  M were prepared for UV-Vis binding studies. The titrant (metal or guest) was sequentially added to a 1 mL sample of the host stock solution in the spectrometric cell and the changes in the spectral features were

monitored. The total number of data points in both NMR and UV-vis experiments were 20–40, depending on the stoichiometry of complexation; for a presumed 1 : 1 complex 20 points were usually measured. The experimental data were fitted to a binding model by the use of the program HYPERQUAD.<sup>45</sup>

### Synthesis

**3,4-Dimethyl-2-N,5-N-bis(2-[(pyridin-2-ylmethyl)amino]phenyl)-1*H*-pyrrole-2,5-dicarboxamide (1).** Zinc perchlorate hexahydrate (416 mg, 1.12 mmol) was added to the solution (methanol 100 ml + toluene 100 ml) of diamine (181 mg, 0.5 mmol) and 2-formylpyridine (107 mg, 1.12 mmol), the mixture were refluxed for 2 h and cooled down to room temperature. Sodium borohydride (*ca.* 4 eq) were added in portions during 30 min until the yellow color of the solution has disappeared. The resulting pale-yellow solution was evaporated, diluted with dichloromethane and washed with saturated aqueous solution of sodium hydrogencarbonate. The organic layer was dried over sodium sulfate and purified by column chromatography (eluent methanol–dichloromethane 10 : 90 v/v, yellow fraction). Yield 130 mg (47%). M.p. 183.4 °C. HRMS calculated for  $C_{32}H_{31}N_4O_2$ ; 545.2539; found: 545.2534.  $^1H$  NMR (300 MHz,  $CDCl_3$ )  $\delta$  11.18 (s, 1H), 8.42 (d,  $J = 4.2$  Hz, 2H), 8.13 (s, 2H), 7.52 (td,  $J = 7.7, 1.7$  Hz, 2H), 7.21 (dd,  $J = 6.8, 4.2$  Hz, 4H), 7.10–6.84 (m, 4H), 6.70–6.44 (m, 4H), 5.16 (d,  $J = 53.3$  Hz, 2H), 4.31 (s, 4H), 2.25 (s, 6H).  $^{13}C$  NMR (75 MHz,  $CDCl_3$ )  $\delta$  157.86, 148.93, 141.37, 136.50, 127.13, 125.57, 124.50, 124.02, 122.26, 121.63, 118.00, 113.12, 105.56, 91.54, 50.35, 49.23, 10.50. ESI-MS(+):  $m/z$   $[M+H]^+$  546.3.

### Zinc complex 2

**1** (100 mg, 0.18 mmol) and  $Zn(ClO_4)_2 \cdot (H_2O)_6$  (68 mg, 0.18 mmol) were mixed in dry methanol (25 ml) and heated to reflux, before being evaporate to dryness. The solid was dissolved in 20 ml of methanol, again heated to reflux and left under r.t. overnight. White crystals are then collected. Yield 80%  $2 \cdot (H_2O)_5 / \text{exp}$  (%calc): C 44.95 (44.97), H 4.29 (4.24), N 11.60 (11.47). M.p. >250 °C decomp. NMR (600 MHz,  $CD_3OD$ )  $\delta$  8.47 (s), 8.07 (td,  $J = 7.8, 1.4$  Hz), 7.83 (d,  $J = 7.9$  Hz), 7.41 (t,  $J = 7.4$  Hz), 7.21 (tt,  $J = 14.6, 11.4$  Hz), 7.04 (d,

$J = 8.1$  Hz), 5.07 (t,  $J = 27.6$  Hz), 2.36 (s).  $^{13}\text{C}$  NMR (101 MHz, MeOD)  $\delta$  162.22, 156.88, 148.48, 142.63, 129.82, 127.89, 126.83, 125.79, 125.57, 125.20, 125.00, 118.28, 118.07, 51.83, 11.28. ESI-MS(+) (in  $\text{CH}_3\text{CN}$ ):  $m/z$  100%  $[\text{I}_2\text{Zn}_2^{4+} + \text{ClO}_4^-]^{3+} - 440.3$ , 20%  $[\text{IZn}^{2+} - \text{H}^+]^+ - 608.3$ , 10%  $[\text{I}_2\text{Zn}_2^{4+} + 2\text{ClO}_4^-]^{2+} 710.3$ .

### X-ray structure determination

Crystal data for  $\text{C}_{71}\text{H}_{80}\text{N}_{14}\text{O}_{27}\text{Zn}_2\text{Cl}_4$ , CCDC 771310  $M = 1844.15$  g mol $^{-1}$ , triclinic,  $P\bar{1}$ ,  $a = 14.7024(4)$  Å,  $b = 15.6663(3)$  Å,  $c = 19.1867(5)$  Å,  $\alpha = 87.631(2)^\circ$ ,  $\beta = 77.559(2)^\circ$ ,  $\gamma = 89.732(2)^\circ$ ,  $V = 4311.81(19)$  Å $^3$ ,  $Z = 2$ , 21330 reflections measured, 14378 independent ( $R_{\text{int}} = 0.0239$ ), which were used in all calculations. The final  $wR_2$  was 0.1729 (all data). Intensity data were collected with a graphite-monochromated Mo-K $\alpha$  radiation ( $\lambda = 1.54184$  Å) at 123 K on a Goniometer Xcalibur, detector: Ruby (Gemini ultra Mo). Data collection, structure solution and refinement used programs: SHELXL,<sup>46</sup> PLATON<sup>47</sup> and SQUEEZE.  $R_1$  is calculated for observed data and  $wR_2$  for all data.

Crystal data for **2** ( $\text{C}_{32}\text{H}_{31}\text{N}_7\text{O}_2 \cdot \text{CH}_4\text{O}$ ), CCDC 789485  $M = 1123.32$  g mol $^{-1}$ , orthorhombic,  $Fdd2$ ,  $a = 24.4639(7)$  Å,  $b = 26.8690(8)$  Å,  $c = 17.3167(4)$  Å,  $V = 11382.6(5)$  Å $^3$ ,  $Z = 8$ , 15515 reflections measured, 4860 independent ( $R_{\text{int}} = 0.0327$ ), which were used in all calculations. The final  $wR_2$  was 0.1151 (all data). Intensity data were collected with a graphite-monochromated Mo-K $\alpha$  radiation ( $\lambda = 1.54184$  Å) at 123 K on a Goniometer Xcalibur, detector: Ruby (Gemini ultra Mo).

### DFT calculations

Molecular modeling calculations were performed using the DFT program "PRIRODA". A PBE functional which includes electron density gradient was used. TZ2p-atomic basis sets of grouped Gaussian functions were used to solve the Kohn–Sham equations. The criterion for convergence was a difference below 0.01 kcal mol $^{-1}$  Å $^{-1}$  in the energy between two sequential structures. Various stationary points on potential energy surface (PES) were determined from analytical calculations of second energy derivatives (Hessian matrixes).

### NMR measurements

NMR spectra were recorded at 300 K on a Bruker Avance DRX 600 (600.13 MHz) and on a Bruker Avance III 600 (600.25 MHz), equipped with a broadband triple-resonance probe and a TCI cryoprobe, respectively. The maximum  $Z$ -gradient field strength of both probes was 53.5 G cm $^{-1}$ . For the NMR diffusion measurements (PFGSE), a stimulated echo sequence using bipolar gradients was applied. NMR data were processed and evaluated with Bruker's TOPSPIN 2.1. and the included t1/t2 software package was used for the calculation of diffusion coefficients.

### Acknowledgements

This work was supported by the Humboldt Foundation. We gratefully acknowledge Prof. Burkhard König for support and

helpful discussions, Sabine Stempfhuber and Dr Manfred Zabel for the X-ray single crystal analysis.

### Notes and references

- 1 P. J. Stang, *J. Org. Chem.*, 2009, **74**, 2–20.
- 2 M. D. Ward, *Chem. Commun.*, 2009, 4487–4499.
- 3 S. L. James, *Chem. Soc. Rev.*, 2009, **38**, 1744–1758.
- 4 E. Zangrando, M. Casanova and E. Alessio, *Chem. Rev.*, 2008, **108**, 4979–5013.
- 5 B. Linton and A. D. Hamilton, *Chem. Rev.*, 1997, **97**, 1669–1680.
- 6 P. Mal, B. Breiner, K. Rissanen and J. R. Nitschke, *Science*, 2009, **324**, 1697–1699.
- 7 R. Warmuth, *Angew. Chem., Int. Ed. Engl.*, 1997, **36**, 1347–1350.
- 8 R. Warmuth and M. A. Marvel, *Angew. Chem., Int. Ed.*, 2000, **39**, 1117–1119.
- 9 M. Yoshizawa, J. K. Klosterman and M. Fujita, *Angew. Chem., Int. Ed.*, 2009, **48**, 3418–3438.
- 10 B. Olenyuk, J. A. Whiteford, A. Fechtenkotter and P. J. Stang, *Nature*, 1999, **398**, 796–799.
- 11 M. D. Levin and P. J. Stang, *J. Am. Chem. Soc.*, 2000, **122**, 7428–7429.
- 12 D. T. de Lill, D. J. Bozzuto and C. L. Cahill, *Dalton Trans.*, 2005, 2111–2115.
- 13 Q. R. Fang, G. S. Zhu, M. Xue, Z. P. Wang, J. Y. Sun and S. L. Qiu, *Cryst. Growth Des.*, 2008, **8**, 319–329.
- 14 L. Q. Ma and W. B. Lin, *J. Am. Chem. Soc.*, 2008, **130**, 13834–13835.
- 15 X. Y. Zhao, D. D. Liang, S. X. Liu, C. Y. Sun, R. G. Cao, C. Y. Gao, Y. H. Ren and Z. M. Su, *Inorg. Chem.*, 2008, **47**, 7133–7138.
- 16 D. K. Bocar, G. S. Papaefstathiou, T. D. Hamilton, Q. L. Chu, I. G. Georgiev and L. R. MacGillivray, *Eur. J. Inorg. Chem.*, 2007, 4559–4568.
- 17 Q. Shi, Y. T. Sun, L. Z. Sheng, K. F. Ma, M. L. Hu, X. G. Hu and S. M. Huang, *Cryst. Growth Des.*, 2008, **8**, 3401–3407.
- 18 R. Vilar, *Eur. J. Inorg. Chem.*, 2008, 357–367.
- 19 M. Yoshizawa, J. Nakagawa, K. Kurnazawa, M. Nagao, M. Kawano, T. Ozeki and M. Fujita, *Angew. Chem., Int. Ed.*, 2005, **44**, 1810–1813.
- 20 M. Yoshizawa, M. Nagao, K. Kumazawa and M. Fujita, *J. Organomet. Chem.*, 2005, **690**, 5383–5388.
- 21 M. A. Galindo, S. Galli, J. A. R. Navarro and M. A. Romero, *Dalton Trans.*, 2004, 2780–2785.
- 22 J. Y. Zhang, P. W. Miller, M. Nieuwenhuyzen and S. L. James, *Chem.–Eur. J.*, 2006, **12**, 2448–2453.
- 23 Z. Grote, R. Scopelliti and K. Severin, *Eur. J. Inorg. Chem.*, 2007, 694–700.
- 24 K. Uehara, K. Kasai and N. Mizuno, *Inorg. Chem.*, 2010, **49**, 2008–2015.
- 25 E. Hollo-Sitkei, G. Tarkanyi, L. Parkanyi, T. Megyes and G. Besenyey, *Eur. J. Inorg. Chem.*, 2008, 1573–1583.
- 26 S. Derossli, M. Casanova, E. Iengo, E. Zangrando, M. Stener and E. Alessio, *Inorg. Chem.*, 2007, **46**, 11243–11253.
- 27 P. S. Mukherjee, K. S. Min, A. M. Arif and P. J. Stang, *Inorg. Chem.*, 2004, **43**, 6345–6350.
- 28 X. F. Huang, K. Nakanishi and N. Berova, *Chirality*, 2000, **12**, 237–255.
- 29 P. Ballester, A. I. Oliva, A. Costa, P. M. Deya, A. Frontera, R. M. Gomila and C. A. Hunter, *J. Am. Chem. Soc.*, 2006, **128**, 5560–5569.
- 30 A. W. Kleij, M. Kuil, D. M. Tooke, M. Lutz, A. L. Spek and J. N. H. Reek, *Chem.–Eur. J.*, 2005, **11**, 4743–4750.
- 31 A. D. Cort, L. Mandolini, C. Pasquini, K. Rissanen, L. Russo and L. Schiaffino, *New J. Chem.*, 2007, **31**, 1633–1638.
- 32 B. König and J. Svoboda, in *Macrocyclic Chemistry: Current Trends and Future Perspectives*, ed. G. Karsten, pp. 87–103.
- 33 V. Amendola, L. Fabbrizzi, P. Pallavicini, L. Parodi and A. Perotti, *J. Chem. Soc., Dalton Trans.*, 1998, 2053–2057.
- 34 V. Amendola, C. Brusoni, L. Fabbrizzi, C. Mangano, H. Miller, P. Pallavicini, A. Perotti and A. Taglietti, *J. Chem. Soc., Dalton Trans.*, 2001, 3528–3533.
- 35 K. Navakhun, P. A. Gale, S. Camiolo, M. E. Light and M. B. Hursthouse, *Chem. Commun.*, 2002, 2084–2085.
- 36 G. W. Bates, P. A. Gale, M. E. Light, M. I. Ogden and C. N. Warriner, *Dalton Trans.*, 2008, 4106–4112.
- 37 C. J. Nyman, E. W. Murbach and G. B. Millard, *J. Am. Chem. Soc.*, 1955, **77**, 4194–4197.

- 38 P. S. Pregosin, P. G. A. Kumar and I. Fernandez, *Chem. Rev.*, 2005, **105**, 2977–2998.
- 39 A. Gierer and K. Z. Wirtz, *Z. Naturforsch. A*, 1953, **8**, 522.
- 40 D. Zuccaccia and A. Macchioni, *Organometallics*, 2005, **24**, 3476–3486.
- 41 D. Benamotz and K. G. Willis, *J. Phys. Chem.*, 1993, **97**, 7736–7742.
- 42 D. N. Laikov and Y. A. Ustynyuk, *Russ. Chem. Bull.*, 2005, **54**, 820–826.
- 43 M. Schmittel and K. Mahata, *Chem. Commun.*, 2008, 2550–2552.
- 44 E. A. Katayev, E. N. Myshkovskaya, N. V. Boev and V. N. Khrustalev, *Supramol. Chem.*, 2008, **20**, 619–624.
- 45 P. Gans, A. Sabatini and A. Vacca, *Talanta*, 1996, **43**, 1739–1753.
- 46 G. M. Sheldrick, *SHELXTL*, v. 6.12, *Structure Determination Software Suite*, (2001) Bruker AXS, Madison, Wisconsin, USA.
- 47 A. L. Spek, (1998) Utrecht University, the Netherlands.